

# Oil-Water Separation Performance of Electrospray Reduced Graphene Oxide Microspheres with a Local Radially Aligned and Porous Structure

YU Ruomeng, SHI Yongzheng and YANG Dongzhi✉

Received March 14, 2021  
Accepted April 14, 2021  
© Jilin University, The Editorial Department of Chemical Research in Chinese Universities and Springer-Verlag GmbH

Micro-size oil adsorbents are effective for the rapid remediation of special oil spills. Here, N-doped reduced graphene oxide(RGO) microspheres(*ca.* 150  $\mu\text{m}$  in diameter) with a local radially aligned and porous structure are fabricated by combining electrospray-freeze-drying with thermal treatment for rapid separation of oil-water. Owing to its hydrophobic/oleophilic properties and oriented structure, the N-doped RGO microspheres achieve high capacities and fast adsorption rates for a variety of oils and organic solvents. Furthermore, excellent oil-water separation performance on floating oil/oil-water emulsions and stable cyclic adsorption capacities are obtained for the local radially aligned and porous microsphere. Therefore, N-doped RGO microspheres with the unique porous structure have the potential for the remediation of oily sewage and oil spills.

**Keywords** Electrospray; Radially aligned structure; Microsphere; Reduced graphene oxide; Oil-water separation

## 1 Introduction

With the rapid development of industrialization, many industries, such as mining, textiles, food industry, petrochemical industry, and metals/steel industry have generated large amounts of oily sewage, which has become a serious global environmental issue<sup>[1,2]</sup>. In addition, frequent oil spills during sea transportation or oil production have caused severe and long-term damage to the marine environment and ecology<sup>[3–8]</sup>. To mitigate and remedy these issues, therefore, the researches for effective adsorption or separation of oil and organic solvent from water have been increasing rapidly<sup>[2,9,10]</sup>. The last few years have seen the development of porous adsorbents<sup>[2,11]</sup>. Among them, hydrophobic and oleophilic materials with ordered structures are promising adsorbents for the adsorption or separation of oil from sewage<sup>[12–14]</sup>.

Porous materials, such as zeolites, sawdust, and wool fibers with a high surface area are currently used for oil absorption<sup>[15]</sup>. Typically, they have high capacities but poor

selectivity for water-oil adsorption<sup>[15]</sup>. State-of-art research shows that microporous polymers with a large specific surface area and hydrophobicity can also be used for oil adsorption<sup>[16,17]</sup>, which obtain relatively high adsorption capacities. But their preparation process is expensive, and their environmental and ecological risks are still unclear. Therefore, it is urgent to develop high-capacity, high-selectivity, and environmentally friendly adsorbents for the adsorption and separation of oil from sewage.

Graphene is a unique two-dimensional(2D) material with tunable interfacial properties<sup>[18,19]</sup>. It has been recognized as a promising material for solving oil spills and pollution problems. Typical graphene-based porous macroscopic materials are three-dimensional(3D) graphene aerogels with super-hydrophobic and super-oleophilic properties<sup>[20–22]</sup>. The micropores and mesopores of 3D graphene aerogel allow the proximity and diffusion of oils and organic solvents, thus acquiring relatively high adsorption performance<sup>[23–26]</sup>. Modulating microstructures, size, and interfacial properties of 3D graphene aerogels would accelerate the adsorption rate and enhance utilization efficiency to remediate special oil spills. For instance, micro-3D graphene aerogels are especially suitable for separating high viscosity or large-area thin spilled oil<sup>[12,27,28]</sup>. Thus, the rational design of chemically functionalized 3D graphene microspheres with oriented structures can further optimize their adsorption performance.

In this work, we prepared N-doped reduced graphene oxide(RGO) microspheres(*ca.* 150  $\mu\text{m}$  in diameter) with a local radially aligned and porous structure by combining electrospray-freeze-drying with thermal treatment for rapid oil-water separation. Owing to the uniform cooling process from the surface to the core of electrospraying microdroplets in the *n*-hexane collector, oriented GO/CS or GO/pDA blocks are constructed through the radial growth of ice crystals. After freeze-drying to remove ice, chitosan(CS) and dopamine(DA) were introduced to chemically functionalize graphene oxide(GO) microspheres. N-Doped RGO microspheres with the oriented and porous structure are fabricated by high-temperature(800  $^{\circ}\text{C}$ ) thermal treatment. The as-prepared

✉ YANG Dongzhi  
yangdz@mail.buct.edu.cn  
Beijing Key Laboratory of Advanced Functional Polymer Composites, College of Materials Science and Engineering, Beijing University of Chemical Technology, Beijing 100029, P. R. China

N-doped RGO microspheres with hydrophobic/oleophilic properties achieve high capacities and fast adsorption rates for varieties of oils and organic solvents. Besides, excellent oil-water separation performance on oil-water emulsions is obtained for the local radially aligned and porous microspheres. Furthermore, the microspheres maintain stable cyclic adsorption capacities.

## 2 Experimental

### 2.1 Materials

Potassium permanganate(KMnO<sub>4</sub>), sodium nitrate(NaNO<sub>3</sub>), ethyl acetate, *n*-hexane, sulfuric acid, *N,N*-dimethylformamide(DMF), and toluene were provided by Beijing Chemical Works(Beijing, China). Graphite flakes were purchased from Huadong Graphite Factory(Pingdu, China). Chitosan(CS) was obtained from Zhejiang Golden-Shell Pharmaceutical Co., Ltd.(Hangzhou, China). Dopamine hydrochloride(DA-HCl) was bought from Acros Organics(USA). Tris-base was provided by Aladdin Chemical Agent Co.(Shanghai, China). Pump oil, lubricating oil, vegetable oil, Oil Red, and sodium dodecylbenzene sulfonate(SDBS) were bought from Hua Gong Special Oil Products Co., Ltd.(Beijing, China), Shell(China) Ltd., Shandong Lu Hua Group Co., Ltd.(China), Alfa Aesar Co., Inc.(China), and Saen Chemical Technology Co., Ltd.(Shanghai, China), respectively.

### 2.2 Preparation of GO/CS and GO/pDA Microspheres

GO was prepared by a modified Hummers' method<sup>[29]</sup>, and the preparation of GO/CS microspheres is detailed in our previous work<sup>[28]</sup>. Typical preparation process of GO/pDA microspheres is described below.

GO(400 mg) was ultrasonically dispersed in 80 mL of deionized water to obtain a homogeneous GO dispersion (5 mg/mL). Tris-base(0.1 g) was added to the GO dispersion to adjust the pH to about 8.0. Then 200 mg of DA-HCl was added, and the DA was polymerized on the surface of the GO sheets to form pDA layers under 300 r/min magnetic stirring for 12 h at room temperature.

The pDA/GO dispersion was placed in a 5 mL syringe and electrospayed using an electrospinning machine. The solid-liquid mixture of liquid nitrogen and ethyl acetate was used to keep the *n*-hexane at -84 °C as a collecting liquid. The droplets ejected from the needle were condensed into ice microspheres in low-temperature *n*-hexane. The electrospaying voltage, the flow rate of the dispersion, and the distance between the needle and collector are +15 kV, 8 mL/h, and 10 cm,

respectively. After electrospaying, ice microspheres were freeze-dried at -20 °C and 20 Pa for 24 h.

### 2.3 Fabrication of N-Doped RGO Microspheres

The as-prepared microspheres were thermally treated in a tube furnace at 800 °C for 3 h in N<sub>2</sub> atmosphere at a heating rate of 5 °C/min. The microspheres prepared from GO/CS dispersions with CS contents of 0, 10%, and 20%(mass fraction) were named RGM-C0, RGM-C10, and RGM-C20, respectively. The microspheres prepared from the GO/pDA dispersion were named RGM-D.

### 2.4 Characterization

The morphology of RGO microspheres was observed with a Hitachi S4700 field emission scanning electron microscope(SEM, Hitachi, Japan). Raman spectra were collected on a Renishaw inVia Raman microscope(Renishaw, UK) at an excitation wavelength of 514 nm. X-Ray photoelectron spectroscopy(XPS) curves were measured on a Thermo VG RSCAKAB 250X high-resolution X-ray photoelectron spectrometer(Thermo, USA). X-Ray diffraction(XRD) patterns were obtained on a Rigaku D/Max 2500 diffractometer with Cu K $\alpha$  radiation(Rigaku, Japan). The static contact angle of the water/oil to the microspheres was performed on a Dataphysics OCA20 contact angle system(Dataphysics, Germany) at room temperature.

### 2.5 Adsorption Experiments

The adsorption performance was tested using three kinds of oil including lubricating oil, pump oil, vegetable oil, and four kinds of organic solvents including toluene, DMF, *n*-hexane, and ethyl acetate as models.

Taking lubricating oil as an example, typical adsorption experiments are as follows: excess lubricating oil was added to  $m_0=50$  mg of microspheres, and the adsorption was saturated in 5 min. The excess oil on the surface of the microspheres was removed with filter paper, and the mass of the microspheres was recorded as  $m_1$ . The adsorption capacity of the microspheres was calculated according to the following equation:

$$q_t = (m_1 - m_0) / m_0 \quad (1)$$

The oil-water separation performance of the microspheres was tested in an oil-water emulsion. The emulsifier SDBS was dispersed in water, then toluene was added and ultrasonically dispersed to obtain the oil/water(O/W) type emulsion with an oil/water volume ratio of 1:10. For visually observing the oil-water separation result by microspheres, the toluene phase was dyed with Oil Red. The N-doped RGO microspheres were

added to the emulsion and magnetically stirred at 200 r/min for 2 min to test its oil-water separation performance.

In order to study the reusability of the adsorbent, the combustion method was adopted to remove the oil adsorbed by the microspheres. After the combustion, the adsorption experiment was repeated.

### 3 Results and Discussion

#### 3.1 Morphology Characterization of N-Doped RGO Microspheres

Typical N-doped RGO microspheres have a hierarchical porous structure with a diameter of approximately 150  $\mu\text{m}$  (Fig.S1, see the Electronic Supplementary Material of this paper). The microspheres are formed by electrospraying, during which the charged GO/CS or GO/pDA suspension droplets are split into microdroplets by high-voltage static electricity and collected in *n*-hexane bath. Owing to the high hydrophobicity and low surface tension of the collector *n*-hexane, the microdroplets turn into ice microspheres with the uniform cooling from the surface to the core, in which radial growth of ice crystals leads to the orientation of GO/CS or GO/pDA blocks<sup>[27,28]</sup>. After freeze-drying to remove ice, the CS or pDA modified GO microspheres are fabricated. Even subjected to thermal treatment, the RGM-C0, RGM-C10, and

RGM-C20 microspheres all possess a relatively complete spherical shape in Fig. 1(A–J). High magnification SEM images of RGM-10 show that the local radially aligned and porous structure is well maintained [Fig.1(G) and (H)], in which RGO layers remain a honeycomb structure and N-doped amorphous carbon retains a cobweb structure. The structural durability of the as-prepared microspheres is mainly attributed to the  $\pi$ - $\pi$  conjugated interaction of the RGO layers and the interconnection of N-doped carbon carbonized from CS<sup>[30]</sup>.

Fig.1(I) and (J) show the SEM images of RGM-D prepared by thermal treatment of GO/pDA composite microspheres. RGM-D forms a flower-like structure of microspheres with randomly distributed RGO sheets on the surface. Different from CS-derived N-doped carbon partially assembled into a cobweb structure between RGO layers in RGM-10, pDA-derived N-doped carbon is mainly distributed on RGO sheets due to the oxidative polymerization and adhesion of pDA.

The XRD patterns of RGO microspheres are shown in Fig.2(A). After thermal treatment, the diffraction peak of GO centered at  $2\theta=11^\circ$  is significantly weakened, and a broad diffraction peak appears at  $2\theta=26.5^\circ$ , indicating that GO is reduced. RGM-C10 and RGM-C20 have broad diffraction peaks compared with RGM-C0, which is ascribed to the disordered distribution of the amorphous carbon formed from

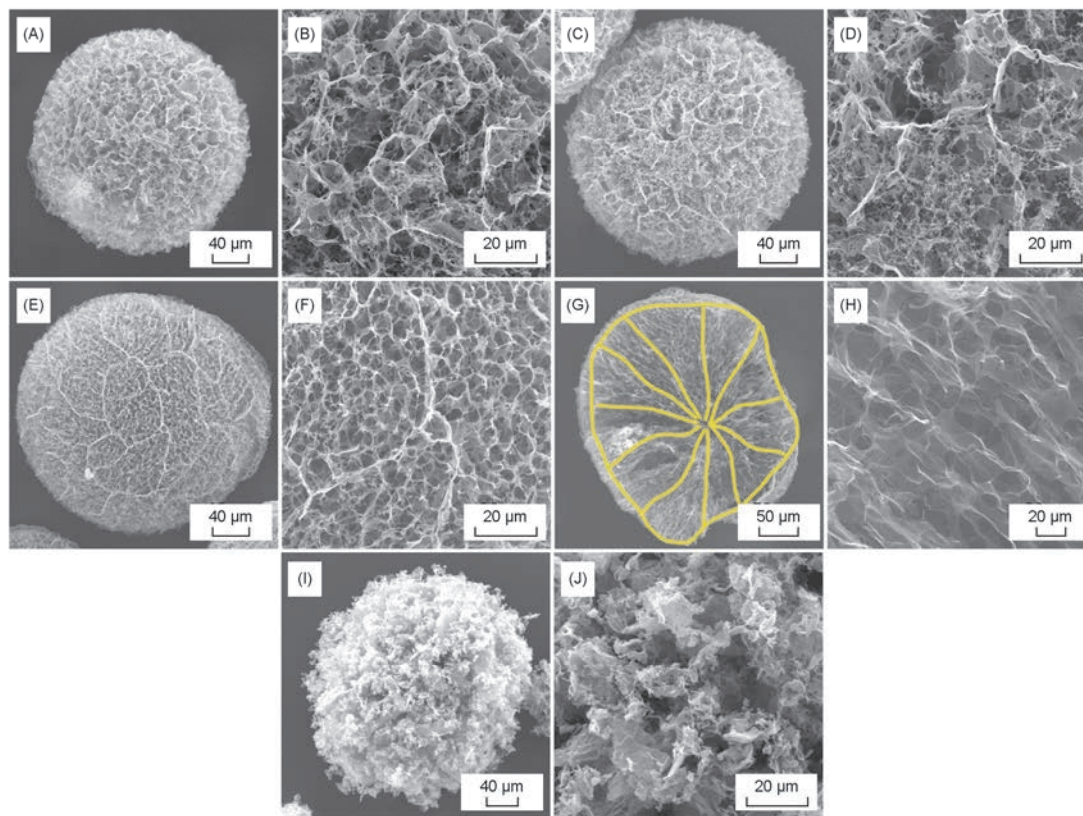
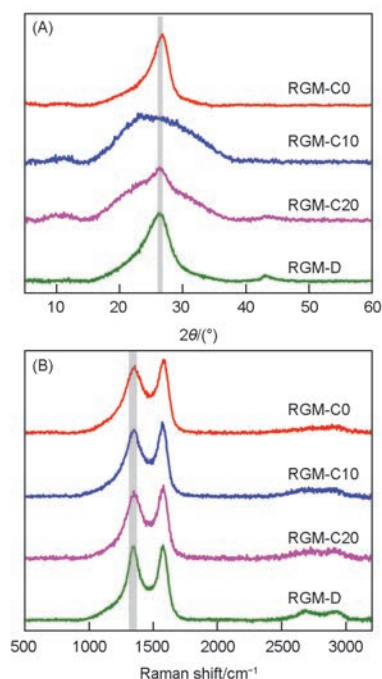


Fig.1 SEM images of RGM-C0(A, B), RGM-C10(C, D), RGM-C20(E, F), and those of the cross-section of RGM-C10(G, H) and RGM-D(I, J) in different magnification

CS. On the other hand, the peak of GO centered at  $2\theta = ca. 10.6^\circ$  disappears after thermal treatment of GO/pDA microspheres, and only one diffraction peak appears at  $ca. 26.2^\circ$ , indicating a higher reduction degree of RGM-D.

Raman spectroscopy is used to evaluate the N-doping degree of graphene. The Raman spectrum of graphene has two main peaks, of which the D peak at  $1300\text{ cm}^{-1}$  reflects structural disorder or defects, and the G peak at  $1580\text{ cm}^{-1}$  represents the  $sp^2$  ordered graphitic carbon region<sup>[28]</sup>. As shown in Fig.2(B),



**Fig.2** XRD patterns(A) and Raman spectra(B) of RGM-C0, RGM-C10, RGM-C20, and RGM-D microspheres

RGM-D has a higher D peak than RGM-C0, RGM-C10, and RGM-C20 due to the substitution of N atoms, which is usually accompanied by the introduction of defects, such as disordered bonding and vacancies in the graphene lattice<sup>[31]</sup>.

The XPS spectra reflect the elemental composition and chemical bonding of the prepared microspheres. Fig.3(A) and (D) show the XPS spectra of RGM-C10 and RGM-D, respectively. The  $N_{1s}$  peak with a binding energy of 402.0 eV indicates that the N element remains in microspheres after thermal treatment at  $800\text{ }^\circ\text{C}$ . The N element contents of RGM-C10 and RGM-D are 4.37% and 4.32% (atomic fraction), respectively. The  $C_{1s}$  peaks of the two microspheres are shown in Fig.3(B) and (E). After partial removal of oxygen-containing functional groups by thermal treatment at  $800\text{ }^\circ\text{C}$ , the C—C bond centered at 284.8 eV becomes the strongest peak<sup>[32]</sup>. The second strongest peak corresponding to the C—N bond at 286.1 eV indicates the successful doping of N element after thermal treatment, which is consistent with XRD and Raman results. The reduction of GO and the carbonization of CS and DA facilitate the formation of hydrophobic surfaces on the microspheres to increase the adsorption capacity of oils and organic solvents. According to the high-resolution XPS curves of  $N_{1s}$  [Fig.3(C) and (F)], the N element has three different chemical bond states: pyridine-N (398.2 eV), pyrrole-N (400.1 eV), and graphite-N (401.1 eV)<sup>[22]</sup>; and the graphite-N ratio of RGM-D is higher than that of RGM-C10. It has been reported that N-doping, especially graphite-N doping, can enhance the  $\pi$ -electron delocalization effect of the graphene sheets, thus significantly increasing the adsorption capacity of the graphene-based material for oil or organic solvents<sup>[21]</sup>.

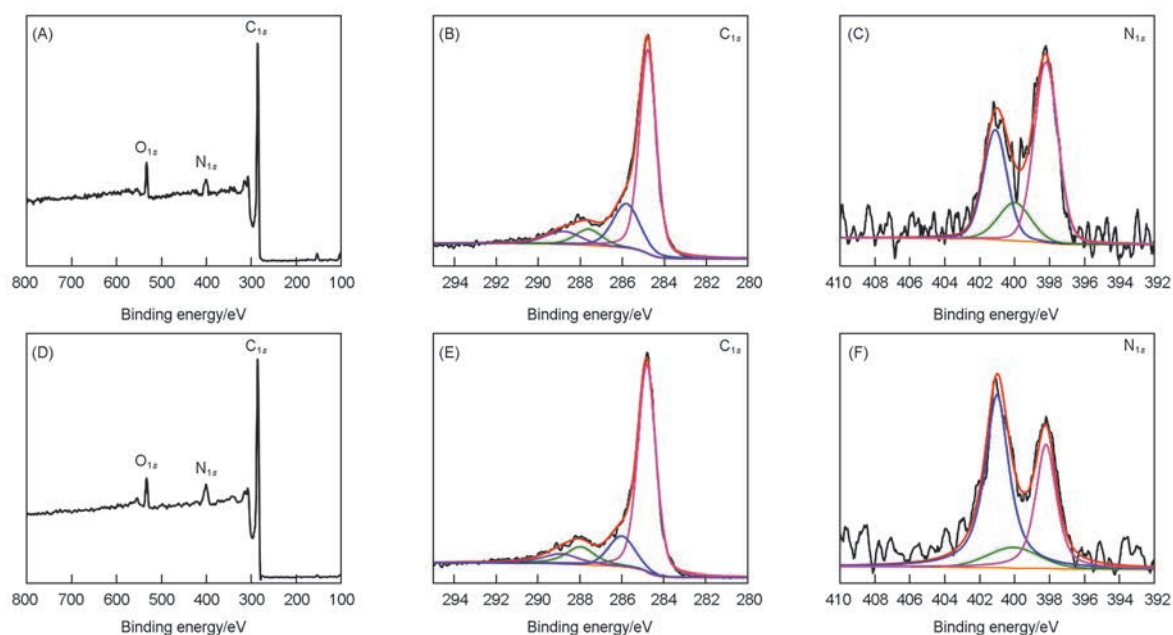


**Fig.3** XPS spectra of RGM-C10(A—C) and RGM-D(D—F)

(A, D) Full survey; (B, E)  $C_{1s}$ ; (C, F)  $N_{1s}$ .

### 3.2 Contact Angle Test

The contact angle is an important method to evaluate the wettability of a liquid to a solid surface. Fig.4(A)—(D) show the hydrophobicity of the four kinds of microspheres by digital images. The contact angles of RGM-C0, RGM-C10, RGM-C20, and RGM-D are 126°, 198°, 215°, and 232°, respectively, which are all higher than 90°, indicating their good hydrophobicity. The high hydrophobicity of RGO microspheres is due to the partial removal of oxygen-containing functional groups after

thermal treatment, as well as the porous microstructure of the microsphere surface. Good hydrophobicity is beneficial to the selective adsorption of oils and non-polar organic solvents.

Fig.4(E—H) show the wettability of lubricating oils for RGO microspheres. The contact angles of RGM-C20 and RGM-D are close to 0°, indicating their excellent wettability for oil. The small contact angles are benefited from the capillary action of the porous microspheres. Hydrophobicity and oleophilicity can speed up the adsorption of microspheres to oils and organic solvents<sup>[33]</sup>.

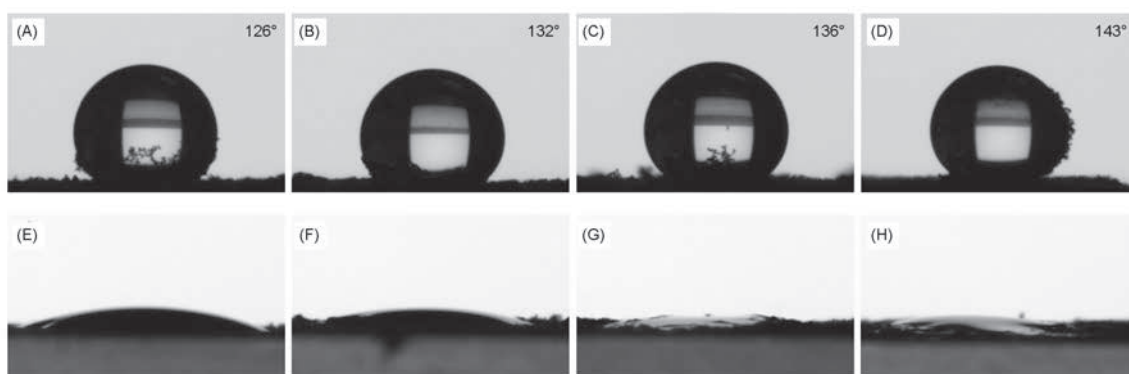


**Fig.4** Wetting behaviors of RGM-C0(A, E), RGM-C10(B, F), RGM-C20(C, G) and RGM-D(D, H) for water(A—D) and lubricating oil(E—H)

### 3.3 Adsorption Performance

The adsorption process of lubricating oil by RGM-C10 is shown in Fig.5. RGM-C10 can quickly adsorb lubricating oils due to the synergistic effect of its micro-size, local radially aligned and porous structure, and hydrophobicity/oleophilicity properties. The fast adsorption performance has advantages in the emergency treatment of crude oil and other chemical spills.

By comparing the adsorption capacities of RGM-C0, RGM-C10, RGM-C20, and RGM-D upon lubricating oil, toluene, and *n*-hexane, we can disclose the influence of N-

doping on the adsorption capacities of the graphene-based microspheres. As the N-doping amount increases in Fig.6(A), the adsorption capacities of microspheres for lubricating oil and *n*-hexane increases slightly, whereas the adsorption capacity of the toluene adsorbent rises significantly. N-Doping has been proven to increase the adsorption capacity of graphene upon oils and organic solvents because N-doped carbon can enhance the plane delocalization  $\pi$  electrons, thus strengthening the adsorption ability of the organic materials, especially benzene-containing organics<sup>[21]</sup>. Fig.6(B) shows the adsorption capacities of RGM-D for several oils and organic solvents, including lubricating oil, pump oil, vegetable oil, toluene, DMF, *n*-hexane, and ethyl acetate. Microspheres have

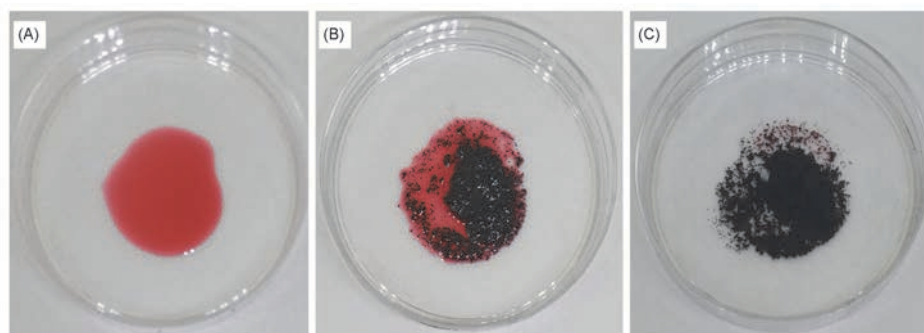


**Fig.5** Removal process of lubricating oil(dyed with Oil Red) using RGM-10 as the adsorbents (A) Before adsorption; (B) adsorbing; (C) after adsorption.

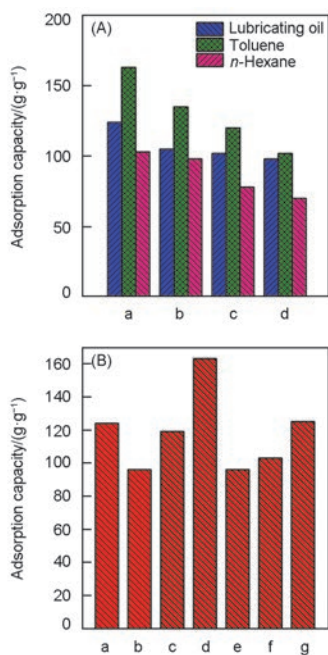


**Fig.6 Adsorbance capacities of the microspheres for lubricating oil, toluene, and *n*-hexane(A) and of RGM-D for oils and organic solvents(B)**

(A) a. RGM-D; b. RGM-C20; c. RGM-C10; d. RGM-C0. (B) a. Lubricating oil; b. pump oil; c. vegetable oil; d. toluene; e. DMF; f. *n*-hexane; g. ethyl acetate.

high adsorption capacities upon these oils and organic solvents. Among them, the adsorption capacity for toluene reached 120.4 g/g owing to the N-doped carbon<sup>[21]</sup>.

Fig.7(A)—(D) show the oil-water separation performance of RGM-C10 microspheres to floating oil. Microspheres have high selectivity and fast adsorption features for the adsorption of floating oil on the water. The microspheres float on the surface of the water after adsorption and can be easily removed. According to the contact angle test, the as-prepared microsphere adsorbent has hydrophobic/oleophilic properties, which significantly accelerate the selective adsorption of oils floating on the water surface.

Some oils form emulsions due to ocean currents in marine oil spill accidents. The removal of these emulsified oils requires adsorbents with a specific pore size. The microspheres have local radially aligned pores ranged from 5  $\mu\text{m}$  to 50  $\mu\text{m}$ , which allow the passage of micro-oil droplets for emulsions. As shown in Fig.7(E—G), the microspheres can absorb the oil in the emulsion, thus achieving oil-water separation.

The microspheres can be recovered by combustion after saturated adsorption[Fig.8(A)]. As shown in Fig.8(B) inset, the used microspheres maintain the porous structure well after burning. The cyclic adsorption capacities of RGM-C10 are

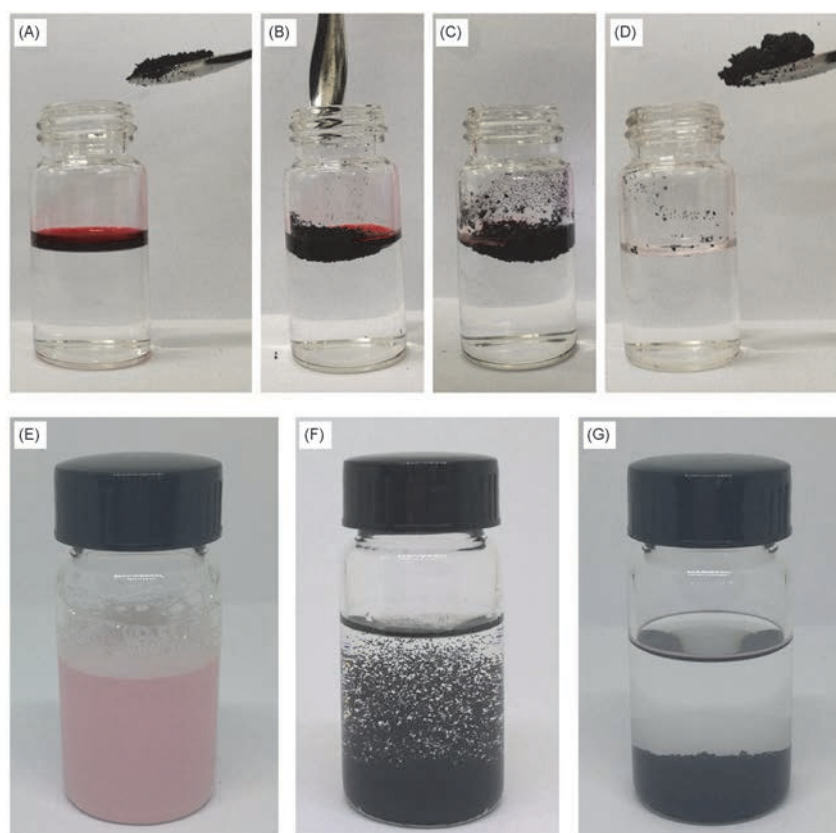


**Fig.7 Removal process of lubricating oil(dyed with Oil Red) in water utilizing RGM-10 as the adsorbent(A—D), and digital pictures of emulsion separation process with RGM-10 as the adsorbents**

(E) The oil-water emulsion before adding microspheres; (F) the oil-water emulsion after adding microspheres; (G) the oil-water separation result of RGM-10 microspheres.

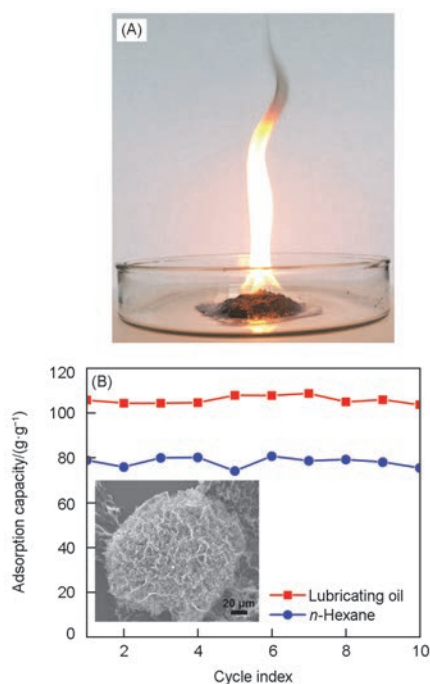


**Fig.8** Combustion process(A) and cyclic utilization of lubricating oil with RGM-C10 serving as the adsorbents(inset, the SEM image of RGM-10 after the 10th adsorption-combustion cycle)(B)

shown in Fig.8(B). After 10 cycles, the microspheres showed a negligible significant capacity loss in the adsorption of lubricating oil and *n*-hexane.

## 4 Conclusions

In conclusion, N-doped reduced graphene oxide(RGO) microspheres(*ca.*150  $\mu\text{m}$  in diameter) with the local radially aligned and porous structure are fabricated by combining electrospray-freeze-drying with thermal treatment for rapid separation of oil-water. CS and DA were introduced as N-source to chemically functionalize graphene oxide(GO) microspheres. Owing to its hydrophobic and oleophilic properties and oriented structure, the N-doped RGO microspheres achieve high capacities and fast adsorption rates for a variety of oils and organic solvents. Furthermore, excellent oil-water separation performance on floating oil/oil-water emulsions and stable cyclic adsorption capacities are obtained for rationally designed microspheres with the unique structure. Therefore, N-doped RGO microspheres have the potential for the remediation of oily sewage and oil spills.

## Electronic Supplementary Material

Supplementary material is available in the online version of this article at <http://dx.doi.org/10.1007/s40242-021-1105-7>.

## Acknowledgements

This work was supported by the National Natural Science Foundation of China(No.51972015).

## Conflicts of Interest

The authors declare no conflicts of interest.

## References

- [1] Chen P. C., Xu Z. K., *Sci. Rep.*, **2013**, 3, 2776
- [2] Ivshina I. B., Kuyukina M. S., Krivoruchko A. V., Elkin A. A., Makarov S. O., Cunningham C. J., Peshkur T. A., Atlas R. M., Philp J. C., *Environ. Sci. Processes Impacts*, **2015**, 17, 1201
- [3] Fu W., Dai Y., Tian J., Huang C., Liu Z., Liu K., Yin L., Huang F., Lu Y., Sun Y., *Nanotechnology*, **2018**, 29, 345607
- [4] Schroppe M., *Nat. News*, **2010**, 466, 680
- [5] Schroppe M., *Nat. News*, **2011**, 472, 152
- [6] McNutt M. K., Camilli R., Crone T. J., Guthrie G. D., Hsieh P. A., Ryerson T. B., Savas O., Shaffer F., *Proc. Natl. Acad. Sci.*, **2012**, 109, 20260
- [7] Jernelöv A., *Nature*, **2010**, 466, 182
- [8] Ryerson T. B., Camilli R., Kessler J. D., Kujawinski E. B., Reddy C. M., Valentine D. L., Atlas E., Blake D. R., de Gouw J., Meinardi S., Parrish D. D., Peischl J., Seewald J. S., Warneke C., *Proc. Natl. Acad. Sci.*, **2012**, 109, 20246
- [9] McNutt M. K., Chu S., Lubchenko J., Hunter T., Dreyfus G., Murawski S. A., Kennedy D. M., *Proc. Natl. Acad. Sci.*, **2012**, 109, 20222
- [10] Joye S. B., *Science*, **2015**, 349, 592
- [11] Guo X., Bi H., Zafar A., Liang Z., Shi Z., Sun L., Ni Z., *Nanotechnology*, **2015**, 27, 055702
- [12] Ge J., Zhao H. Y., Zhu H. W., Huang J., Shi L. A., Yu S. H., *Adv. Mater.*, **2016**, 28, 10459
- [13] Wang S., Song Y., Jiang L., *Nanotechnology*, **2006**, 18, 015103
- [14] Wang S., Liu K., Yao X., Jiang L., *Chem. Rev.*, **2015**, 115, 8230
- [15] Liu S., Xu Q., Latthe S. S., Gurav A. B., Xing R., *RSC Adv.*, **2015**, 5, 68293
- [16] Zhu Q., Pan Q., Liu F., *J. Phys. Chem. C*, **2011**, 115, 17464
- [17] Zhang X., Li Z., Liu K., Jiang L., *Adv. Funct. Mater.*, **2013**, 23, 2881
- [18] Kharissova O. V., Dias H. R., Kharisov B. I., *RSC Adv.*, **2015**, 5, 6695
- [19] Kong Z., Wang J., Lu X., Zhu Y., Jiang L., *Nano Res.*, **2017**, 10, 1756
- [20] Li J., Li J., Meng H., Xie S., Zhang B., Li L., Ma H., Zhang J., Yu M., *J. Mater. Chem. A*, **2014**, 2, 2934
- [21] Zhao Y., Hu C., Hu Y., Cheng H., Shi G., Qu L., *Angew. Chem. Int. Ed.*, **2012**, 51, 11371
- [22] Song X., Lin L., Rong M., Wang Y., Xie Z., Chen X., *Carbon*, **2014**, 80, 174
- [23] Yang S., Chen L., Mu L., Ma P. C., *J. Colloid Interface Sci.*, **2014**, 430, 337
- [24] Liu C., Yang J., Tang Y., Yin L., Tang H., Li C., *Colloids Surf. A*, **2015**, 468, 10
- [25] Wan W., Zhang R., Li W., Liu H., Lin Y., Li L., Zhou Y., *Environ. Sci.: Nano*, **2016**, 3, 107
- [26] Chen L., Du R., Zhang J., Yi T., *J. Mater. Chem. A*, **2015**, 3, 20547
- [27] Liao S., Zhai T., Xia H., *J. Mater. Chem. A*, **2016**, 4, 1068
- [28] Yu R., Shi Y., Yang D., Liu Y., Qu J., Yu Z. Z., *ACS Appl. Mater. Interfaces*, **2017**, 9, 21809
- [29] Hummers W. S., Offeman R. E., *J. Am. Chem. Soc.*, **1958**, 80, 1339
- [30] Xu K., Chen G., Qiu D., *J. Mater. Chem. A*, **2013**, 1, 12395
- [31] Panchakarla L. S., Subrahmanyam K. S., Saha S. K., Govindaraj A., Krishnamurthy H. R., Waghmare U. V., Rao C. N. R., *Adv. Mater.*, **2009**, 21, 4726
- [32] Wan S., Peng J., Li Y., Hu H., Jiang L., Cheng Q., *ACS Nano*, **2015**, 9, 9830
- [33] Wang B., Liang W., Guo Z., Liu W., *Chem. Soc. Rev.*, **2015**, 44, 336